



Nonlinearity compensation using optical phase conjugation deployed in discretely amplified transmission systems

MOHAMMAD A. Z. AL-KHATEEB,^{1,*} MARY E. MCCARTHY,^{1,2} CHRISTIAN SÁNCHEZ,¹ AND ANDREW D. ELLIS¹

¹Aston Institute of Photonic Technologies (AIPT), Aston University, Birmingham B4 7ET, UK

²Now with Oclaro Technologies, Long Road, Paignton TQ4 7AU, UK

*alkhamaz@aston.ac.uk

Abstract: We introduce a closed form equation, validated by simulations and experimental results that predicts the residual nonlinear noise ratio in mid-link OPC assisted discretely amplified systems. The model anticipates the reduction in performance enhancement achieved by mid-link OPC as the bandwidth of the modulated signals increases. The numerical analysis shows that uncompensated signal-signal interactions limit the performance improvement achieved by the introduction of additional OPCs. The numerical analysis predicts that the deployment of shorter amplifier spacing will lead to a greater performance enhancement. The numerical results are validated by experimentally testing of 2x, 4x, and 8x28Gbaud PM-QPSK systems with mid-link OPC compensation in a discretely amplified system with 100km amplifier spacing. The experimentally obtained reach enhancement (43%, 32%, and 24% for 2x28Gbaud, 4x28Gbaud, and 8x28Gbaud, respectively) confirms that the compensation efficiency of mid-link OPC is highly dependent on the number of channels (bandwidth) propagating along the system.

Published by The Optical Society under the terms of the [Creative Commons Attribution 4.0 License](https://creativecommons.org/licenses/by/4.0/). Further distribution of this work must maintain attribution to the author(s) and the published article's title, journal citation, and DOI

OCIS codes: (060.4510) Optical communications; (070.5040) Phase conjugation; (190.4370) Nonlinear optics, fibers.

References and links

1. A. Yariv, D. Fekete, and D. M. Pepper, "Compensation for channel dispersion by nonlinear optical phase conjugation," *Opt. Lett.* **4**(2), 52 (1979).
2. W. Shieh and Xi Chen, "Information spectral efficiency and launch power density limits due to fiber nonlinearity for coherent optical OFDM systems," *IEEE Photonics J.* **3**(2), 158–173 (2011).
3. K. O. Hill, D. C. Johnson, B. S. Kawasaki, and R. I. MacDonald, "Cw three-wave mixing in single-mode optical fibers," *J. Appl. Phys.* **49**(10), 5098–5106 (1978).
4. A. D. Ellis and W. A. Stallard, "Four wave mixing in ultra long transmission systems incorporating linear amplifiers," in *IEE Colloquium on Non-Linear Effects in Fibre Communications*. p. 6/1–6/4, 1990.
5. K. Inoue, "Phase-mismatching characteristic of four-wave mixing in fiber lines with multistage optical amplifiers," *Opt. Lett.* **17**(11), 801–803 (1992).
6. S. Radic, G. Pendo, A. Srivastava, P. Wysocki, and A. Chraplyvy, "Four-wave mixing in optical links using quasi-distributed optical amplifiers," *J. Lightwave Technol.* **19**(5), 636–645 (2001).
7. M. A. Z. Al-Khateeb, M. A. Iqbal, M. Tan, A. Ali, M. McCarthy, P. Harper, and A. D. Ellis, "Analysis of the nonlinear Kerr effects in optical transmission systems that deploy optical phase conjugation," *Opt. Express* **26**(3), 3145–3160 (2018).
8. A. D. Ellis, M. E. McCarthy, M. A. Z. Al Khateeb, M. Sorokina, and N. J. Doran, "Performance limits in optical communications due to fiber nonlinearity," *Adv. Opt. Photonics* **9**(3), 429–503 (2017).
9. M. E. McCarthy, M. A. Z. Al Kahteeb, F. M. Ferreira, and A. D. Ellis, "PMD tolerant nonlinear compensation using in-line phase conjugation," *Opt. Express* **24**(4), 3385–3392 (2016).
10. D. Rafique and A. D. Ellis, "Impact of signal-ASE four-wave mixing on the effectiveness of digital back-propagation in 112 Gb/s PM-QPSK systems," *Opt. Express* **19**(4), 3449–3454 (2011).
11. M. A. Z. Al-Khateeb, M. McCarthy, C. Sánchez, and A. Ellis, "Effect of second order signal-noise interactions in nonlinearity compensated optical transmission systems," *Opt. Lett.* **41**(8), 1849–1852 (2016).
12. A. D. Ellis, M. E. McCarthy, M. A. Z. Al-Khateeb, and S. Sygletos, "Capacity limits of systems employing multiple optical phase conjugators," *Opt. Express* **23**(16), 20381–20393 (2015).

13. M. A. Z. Al-Khateeb, M. E. McCarthy, and A. Ellis, "Performance enhancement prediction for optical phase conjugation in systems with 100km amplifier spacing," in *Proc. European Conference and Exhibition on Optical Communication (ECOC)* (2017), p. Th.1.F.4.
14. K. Solis-Trapala, M. Pelusi, H. N. Tan, T. Inoue, and S. Namiki, "Optimized WDM transmission impairment mitigation by multiple phase conjugations," *J. Lightwave Technol.* **34**(2), 431–440 (2016).
15. H. Hu, R. M. Jopson, A. H. Gnauck, S. Randel, and S. Chandrasekhar, "Fiber nonlinearity mitigation of WDM-PDM QPSK/16-QAM signals using fiber-optic parametric amplifiers based multiple optical phase conjugations," *Opt. Express* **25**(3), 1618–1628 (2017).
16. E. Desurvire, *Erbium Doped Fiber Amplifiers: Principles and Applications*, John Wiley & Sons, N.Y., 1994.
17. M. H. Shoreh, "Compensation of nonlinearity impairments in coherent optical OFDM systems using multiple optical phase conjugate modules," *J. Opt. Commun. Netw.* **6**(6), 549–558 (2014).
18. R.-J. Essiambre, G. Kramer, P. J. Winzer, G. J. Foschini, and B. Goebel, "Capacity limits of optical fiber networks," *J. Lightwave Technol.* **28**(4), 662–701 (2010).
19. A. D. Ellis and N. J. Doran, "Optical link design for minimum power consumption and maximum capacity," in *39th European Conference and Exhibition on Optical Communication (ECOC 2013)* (Institution of Engineering and Technology, 2013), pp. 1068–1070.
20. P. Poggiolini, "The GN model of non-linear propagation in uncompensated coherent optical systems," *J. Lightwave Technol.* **30**(24), 3857–3879 (2012).
21. S. Yoshima, Y. Sun, Z. Liu, K. R. H. Bottrill, F. Parmigiani, D. J. Richardson, and P. Petropoulos, "Mitigation of nonlinear effects on WDM QAM signals enabled by optical phase conjugation with efficient bandwidth utilization," *J. Light. Technol.* **35**, 971 (2017).
22. M. Morshed, L. B. Du, B. Foo, M. D. Pelusi, B. Corcoran, and A. J. Lowery, "Experimental demonstrations of dual polarization CO-OFDM using mid-span spectral inversion for nonlinearity compensation," *Opt. Express* **22**(9), 10455–10466 (2014).
23. I. Phillips, M. Tan, M. F. Stephens, M. McCarthy, E. Giacomidis, S. Sygletos, P. Rosa, S. Fabbri, S. T. Le, T. Kanesan, S. K. Turitsyn, N. J. Doran, P. Harper, and A. D. Ellis, "Exceeding the nonlinear-Shannon limit using Raman laser based amplification and optical phase conjugation," in *Optical Fiber Communication Conference* (2014), p. M3C.1.
24. I. Sackey, F. Da Ros, J. Karl Fischer, T. Richter, M. Jazayerifar, C. Peucheret, K. Petermann, and C. Schubert, "Kerr nonlinearity mitigation: mid-link spectral inversion versus digital backpropagation in 5×28-GBd PDM 16-QAM signal transmission," *J. Lightwave Technol.* **33**(9), 1821–1827 (2015).
25. I. Sackey, R. Elschner, C. Schmidt-Langhorst, T. Kato, T. Tanimura, S. Watanabe, T. Hoshida, C. Schubert, and C. Schubert, "Novel wavelength-shift-free optical phase conjugator used for fiber nonlinearity mitigation in 200-Gb/s PDM-16QAM transmission," in *Optical Fiber Communication Conference (OSA, 2017)*, p. Th3J.1.

1. Introduction

The accumulation of amplified spontaneous emission noise and nonlinear Kerr effects along optical fiber transmission systems determine the performance limit of the modulated signals propagating through these systems. Optical phase conjugation (OPC) [1] is a promising nonlinearity compensation technique, but the achievable nonlinearity compensation efficiency is highly dependent on the link properties. The calculation of nonlinear noise limit in optical transmission systems [2] requires performing double integration, over the modulated signal bandwidth, of the power of the nonlinear products resulting from the interaction of (up to) three optical spectral tones [3–7]. The analytical representation of nonlinear product has been studied in various optical transmission systems, such as: single span systems [3], multi-span discretely amplified systems [4], dispersion managed discretely amplified systems [5], distributed Raman systems [6], and OPC assisted discretely (and distributed Raman) amplified systems [7]. An ideal OPC assisted system (deployed in an ideal lossless Raman system) should fully compensate the deterministic nonlinear interactions between different signal frequencies to reach a new nondeterministic nonlinear noise limit [8] (from either polarization mode dispersion [PMD] [9], or interaction between signal and noise [10, 11]). In such ideal systems, the deployment of multiple OPCs lead to the reduction of these nondeterministic nonlinear interactions [12]. However, OPC assisted systems may also be limited by uncompensated deterministic nonlinear signal-signal interactions due to, for example, the lack of signal power symmetry, especially with large amplifier spacing's [13]; in such case increasing the number of OPCs may even degrade the performance of the modulated optical signals due to additional linear noise [14, 15]. In order to optimize the number of OPCs in a given link, it thus necessary to understand the trade-off between

incompletely compensated intra signal nonlinearity, and reduced signal-noise nonlinear interactions.

In this paper, we present a theoretical analysis, verified by simulation and experimental results, to quantify the achievable performance enhancement when OPCs are deployed in discretely amplified transmission systems, extending our prior work [13] to highlight the influence of amplifier spacing. We show that the nonlinearity compensation efficiency achieved by mid-link OPC is highly dependent on the total bandwidth of the optical modulated signals as well as the amplifier spacing (span length) across the system. We also show that the deployment of multiple OPCs in a system can diminish the intra signal nonlinearity compensation efficiency compared to that of a single, mid-link, OPC, due to the inherent dispersion compensation capabilities of the OPC. Finally, experimental results obtained from 2x, 4x, and 8x28Gbaud PM-QPSK systems with mid-link OPC are presented, showing a reach enhancement of 43%, 32%, and 24% for 2x28Gbaud, 4x28Gbaud, and 8x28Gbaud, respectively, verifying the bandwidth dependence of the performance gain in excellent agreement with a closed form expression that predicts the dependency of the residual nonlinearities in OPC assisted discretely amplified system as a function of bandwidth (within 0.3dB margin of error).

2. Theoretical evaluation

The signal to noise ratio (SNR) of the received optical signal propagating through a uniform discretely amplified optical transmission system can be written as:

$$SNR = \frac{I_s}{NI_{ASE} + \kappa I_s^3 \eta_{ss}(N) + 3I_s^2 I_{ASE} \eta_{sn}(N)}, \quad (1)$$

where I_s is the power spectral density of the modulated signals, N is the number of inline optical amplifiers and number of spans, I_{ASE} is the power spectral density of amplified spontaneous emission (ASE) noise generated from each optical amplifier, $\eta_{ss}(N)$ is the nonlinear noise generation efficiency due signal-signal interactions for N spans, κ is the residual nonlinear noise ratio in the OPC assisted system (compared to a system without OPC), and $\eta_{sn}(N)$ is the nonlinear noise generation efficiency due to signal-noise interactions for N spans. In EDFA-amplified systems, I_{ASE} is given by [16]:

$$NI_{ASE} = \frac{NP_{ASE}}{B_w} = 2n_{sp} h\nu N(G-1) \quad (2)$$

where G is the gain provided by each EDFA (compensating for the optical span loss, $\exp(\alpha L)$, where α is the optical fibers' attenuation constant and L is the span length), h is the Planck constant, ν is the optical frequency, and n_{sp} is the spontaneous emission factor. The nonlinear signal-signal noise generation efficiency ($\kappa\eta_{ss}$, see Eq. (1)) is highly dependent on the properties of the transmission system and the number of OPCs deployed symmetrically along the link. For dispersion uncompensated discretely amplified system (N spans without OPC, $\kappa = 1$), its value can be calculated from the double integration of the nonlinear mixing efficiency [4] over the full bandwidth of the modulated wavelength division multiplexed (WDM) signals [2] (B_w) (assuming spectrally efficient Nyquist-WDM signals with baud rate approximately equal to the spectral spacing between the WDM channels) as follows:

$$\eta_{ss}(N) = 3\gamma^2 \int_0^{B_w/2} \int_0^{B_w/2} \left[\frac{\alpha^2 L_{eff}^2}{\alpha^2 + \Delta\beta^2} \right] \left[1 + \frac{4e^{(-\alpha L)} \sin^2(\Delta\beta L / 2)}{(1 - e^{(-\alpha L)})^2} \right] \left[\frac{\sin^2(\Delta\beta NL / 2)}{\sin^2(\Delta\beta L / 2)} \right] df_1 df_2. \quad (3)$$

Whilst for an OPC assisted system, the net generation efficiency is calculated for N spans, as follows [7]:

$$\kappa\eta_{ss}(N) = 3\gamma^2 N_{seg}^2 \int_0^{B_w/2} \int_0^{B_w/2} \left[\frac{\alpha(e^{-\alpha L} + 1) \sin(\Delta\beta L / 2) + \alpha\Delta\beta L_{eff} \cos(\Delta\beta L / 2)}{\alpha^2 + \Delta\beta^2} \right]^2 \left[\frac{\sin^2(\Delta\beta NL / [2N_{seg}])}{\sin^2(\Delta\beta L / 2)} \right] df_1 df_2, \quad (4)$$

where $\Delta\beta$ is the phase matching factor determined by the mixing signal frequencies (f_1 and f_2) and the second order propagation constant β'' ($\Delta\beta = 4\pi^2\beta''f_1f_2$), L_{eff} is the fiber effective length ($L_{eff} = [1 - \exp(-\alpha L)]/\alpha$), γ is the nonlinear coefficient, and N_{seg} is the number of segments in OPC assisted system. Symmetrical deployment of the OPC(s) divides the optical transmission link into segments where the propagation of signals within an even indexed segment ideally compensates for the nonlinearities accumulated along the previous odd indexed segment. There are two common approaches reported to deploy multiple OPCs along a link: single segment spaced OPCs where the number of spans between signal processing elements (transmitters, OPCs and receivers) are equal [12], and double segment spaced OPCs where the number of spans between the transmitter/receiver and the nearest OPC is half the number of spans between two consecutive OPCs [17]. For notational convenience we consider that the number of segments with single segment spaced OPCs is $N_{seg} = N_{OPC} + 1$ [number of spans per segment = $N/(N_{OPC} + 1)$], whilst the number for double segment spacing is $N_{seg} = 2N_{OPC}$ [number of spans per segment = $N/(2N_{OPC})$]. This definition implies that for a system with fixed number of spans, higher number of OPCs (N_{OPC}) results in a higher number of segments and smaller number of spans per segment. Figure 1 shows the definition of “segments” in multi-OPC assisted system that has four segments, where the even indexed segment ought to compensate for the nonlinearities accumulated along the previous odd indexed segment. The figure shows the difference between the single spaced OPCs [Fig. 1(a)], and the double segment spaced OPCs [Fig. 1(b)]. It can be seen from the figure that the double segment spaced OPCs requires lower number of OPCs (two in this case) when compared to the single segment spaced OPCs (three in this case), since the double segment spaced OPC deployment omits the OPCs located at zero dispersion accumulation (dispersion free) points along the link. As the signal power profile is the same in both configurations, then the nonlinearities occurring in both configurations are similar and can be represented by Eq. (4) which was concluded by the analytical analysis in [7].

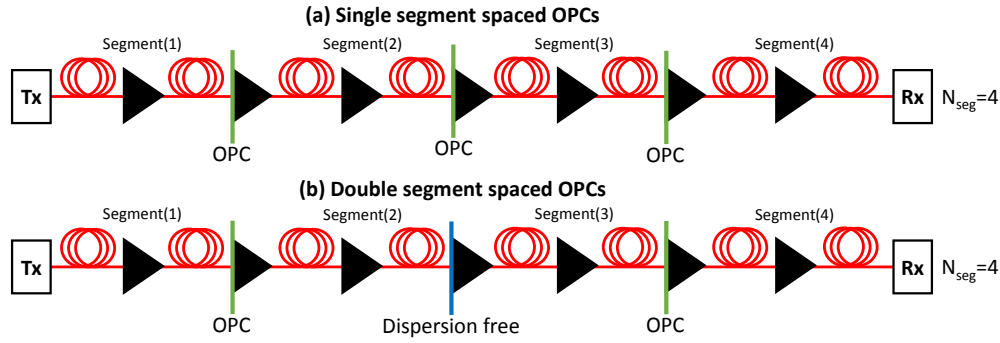


Fig. 1. Definition of segments in OPC assisted optical transmission systems. (a) Single segment spaced OPCs, (b) double segment spaced OPCs.

As may be seen from Eq. (4) an OPC may fully compensate for the nonlinear interactions among strongly phase matched signals (signals with low frequency separation, $\Delta\beta \ll \alpha$) as both terms in the first squared brackets have negligible value. However, the net nonlinear noise generation efficiency for weakly phase matched signals (signals with high frequency separation, $\Delta\beta \gg \alpha$) will converge to that of a system without OPC [7] except for the quasi-phase matching term (second square bracketed term in Eq. (4)). This term represents quasi-phase matching between both spans and segments representing a highly oscillatory (as a function of $\Delta\beta$) scaling factor. In the same way that adding dispersion compensating fiber to dispersion managed system increases quasi-phase matching, deployment of multiple OPCs (increasing N_{seg}) also increases quasi-phase matching, and effectively reduces the oscillation frequency (as a function of $\Delta\beta$) of the quasi-phase matching peaks, as described by last term in the integration in Eq. (4). This implies a slight enhancement in the nonlinear noise generation efficiency as a function of number of OPCs [7].

The nonlinear noise generation efficiency of a uniform discretely amplified system [without OPC, Eq. (3)] can be approximated assuming long span length ($\exp(-\alpha L) \ll 1$, $L_{eff} = 1/\alpha$) to [2]:

$$\eta_{ss}(N) = \frac{3\gamma^2 N}{8\pi|\beta^n|\alpha} \log\left(\frac{2\pi^2|\beta^n|B_w^2}{\alpha}\right). \quad (5)$$

With the same span length approximation, the residual nonlinear noise ratio (κ) for a system deploying mid-link OPC can be simplified as [13]:

$$\begin{aligned} \kappa &\approx \frac{4}{B_w^2} \int_0^{B_w/2} \int_0^{B_w/2} \frac{(4\pi^2\beta^n f_1 f_2)^2}{\alpha^2 + (4\pi^2\beta^n f_1 f_2)^2} df_1 df_2 \\ &\approx 1 - \frac{2\alpha}{\pi^2|\beta^n|B_w^2} \text{a sinh}\left(\frac{\pi^2|\beta^n|B_w^2}{2\alpha}\right). \end{aligned} \quad (6)$$

The residual nonlinearity ratio is approximated by performing the normalized double integration (over the full WDM bandwidth) of the *simplified* ratio between nonlinear Kerr power resulted in OPC assisted system and the nonlinear Kerr power resulted in a system without OPC ($\Delta\beta^2/[\alpha^2 + \Delta\beta^2]$). The simplified ratio [Eq. (6)] represents the residual nonlinear noise ratio among the strongly matched signals and ignores weakly phase matched signal, as no nonlinearity compensation is expected to be formed among them [13]. The minor nonlinear Kerr product power oscillations resulted from strongly phase matched signals (as $N_{seg} \sin(\Delta\beta NL/[2N_{seg}])/\sin(\Delta\beta NL/2) \approx 1$, as $\Delta\beta \rightarrow 0$ [13]) were ignored in the derivation of Eq. (6). Equation (6) shows a clear relation between the residual nonlinearities ratio and optical

fiber parameters (α and β'') as well as the bandwidth of the modulated signals propagating along the system. κ reaches its maximum value ($\kappa = 1$) at large bandwidth (higher number of WDM modulated signals) as the uncompensated weakly phase matched nonlinear interference dominates over the compensated strongly phase matched nonlinear interference. When deploying a mid-link OPC, the residual nonlinear noise ratio (κ) can be minimized, aside from reducing the signal bandwidth B_w , by deploying optical fiber spans that has lower attenuation and dispersion coefficients (α and β''). Equation (6) shows that deploying lossless ($\alpha = 0$) or dispersion-less ($\beta'' = 0$) optical fiber spans enables the OPC to achieve full signal-signal nonlinearity compensation ($\kappa = 0$). Such systems can be realized by deploying quasi-lossless distributed Raman amplification, or dispersion shifted fiber spans; at which the deployment of OPC fully compensate the signal-signal nonlinear interactions ($\kappa = 0$) but the system will still be limited by the signal-noise nonlinear interactions [the third term in the denominator of Eq. (1)] [10, 11].

Looking back to Eq. (1), achieving sufficiently low κ value by (deploying OPC) results a reduction in the signal-signal nonlinear interactions (which enhances SNR), but the system will still be limited by the nonlinear interactions between the signals and the ASE noise. The net nonlinear noise generation efficiency of signal-noise interactions [$\eta_{sn}(N)$] can be written for a transmission system that deploys N discretely amplified spans (with N amplifiers) as [11,12]:

$$\eta_{sn}(N) = N_{seg} \left[\sum_{n=1}^{N/N_{seg}} \eta_{ss}(n) + 3I_s^2 \eta_{ss}(1) \sum_{n=1}^{N/N_{seg}} \sum_{i=1}^{n-1} \eta_{ss}(i) \right], \quad (7)$$

where $\eta_{ss}(x)$ refers to the nonlinear signal-signal noise generation efficiency from x spans [which is defined in Eq. (4)]. The expression presented in Eq. (7) can be approximated for large amplifier spacing as [11]:

$$\eta_{sn}(N) = \frac{3\gamma^2 \frac{N}{N_{seg}} \left(\frac{N}{N_{seg}} + 1 \right)}{8\pi\alpha|\beta'|} \log \left(\frac{2\pi^2 |\beta''| B_w^2}{\alpha} \right) \left[1 + \frac{9\gamma^2 I_s^2 \left(\frac{N}{N_{seg}} - 1 \right)}{8\pi\alpha|\beta'|} \log \left(\frac{2\pi^2 |\beta''| B_w^2}{\alpha} \right) \right]. \quad (8)$$

The finite residual value for the nonlinear signal-noise interactions arises from the fact that different ASE noise fields is added from each amplifier along the link. The asymmetric propagation of modulated signals and each ASE noise field (in reference to the deployed OPC) results an over/ or under/ compensation of the nonlinear interaction between each ASE noise field and the signal; graphical analysis of the evolution of these nonlinearities can be found in [8, 10, 11]. $\eta_{sn}(N)$ consists of the 1st order signal-noise nonlinear interactions [represented by the first term in the squared brackets in Eq. (7) and Eq. (8)] as well as the 2nd order signal-noise nonlinear interactions [represented by the second term in the squared brackets in Eq. (7) and Eq. (8)] [11]. Both equations show that the deployment of multiple OPCs along the system (increasing N_{seg}) would result a reduction of the 1st order signal-noise nonlinear interactions by a factor of $(1/N_{seg})^2$ as well as a reduction of the 2nd order signal-noise nonlinear interactions by a factor of $(1/N_{seg})^3$. This indicates that increasing the number of deployed OPCs (in a system that has $\kappa = 0$) would result in a reduction in $\eta_{sn}(N)$ leading to the enhancement of SNR [see Eq. (1)] [10, 11].

3. Simulation results and numerical analysis

Simulations of a single channel 28Gbaud PM-QPSK systems were performed in order to quantify the performance improvement achieved by OPC assisted discretely amplified systems compared to an Electronically Dispersion Compensated (EDC) system. The total length of the simulated link was 2400km of standard single mode fiber ($L = 100\text{km}$, $\gamma =$

1.3/W/km, $\alpha = 0.2\text{dB/km}$, chromatic dispersion (CD) = 16ps/nm/km), and different sets of simulations were undertaken for different values of amplifier spacing: ranging from 100km to 6.25km. The EDFAs used in the simulations had a spontaneous emission factor (n_{sp}) of 1.085 (noise figure = 3.36dB) the systems used either 0, 1, 2, or 3 symmetrically deployed ideal lossless OPCs with double segmented spacing. The simulations were conducted in VPITransmissionMaker v9.8 which uses simulation bandwidth of 896GHz and solves the split step Fourier where the step size is defined so that the total nonlinear phase shift within the step is always less than 0.05° . MATLAB was used to generate 28Gbaud PM-QPSK (Nyquist pulse shaped with 0% roll-off factor) signals and perform DSP on the coherently received signals. Figure 2 shows the simulation results (filled dots) and the analytical prediction (solid lines) of the system performance (Q^2 factor = $1/EVM^2$) of 28Gbaud PM-QPSK (where $Q^2 = SNR$ [8]) as a function of the signal power launched into the system. The analytically predicted nonlinear noise generation efficiencies were numerically calculated from Eq. (3), Eq. (4), and Eq. (7), whilst Eq. (1) was to calculate the SNR (or Q^2) of the received signal.

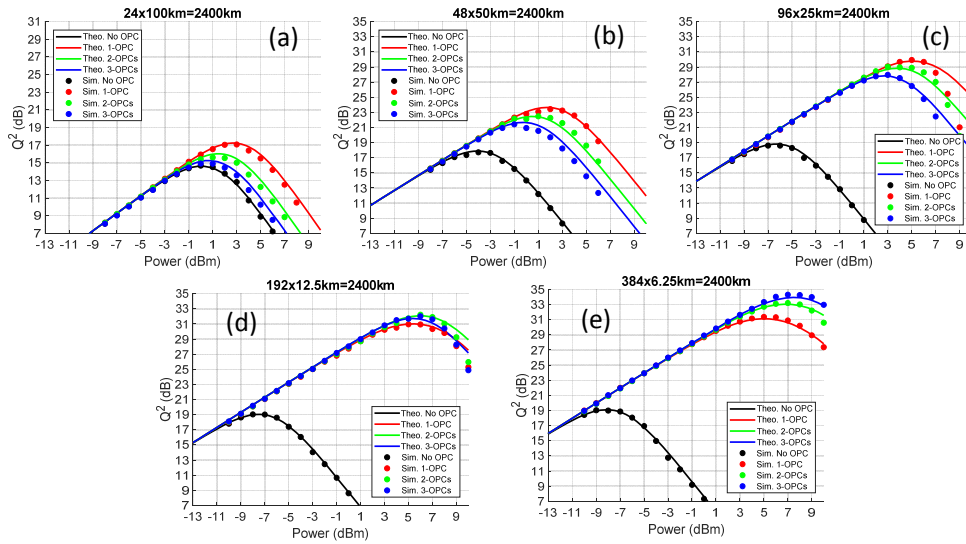


Fig. 2. Q^2 as a function of signal power for discretely amplified 2400km transmission system with uniform amplifier spacing of: (a) 24x100km, (b) 48x50km, (c) 96x25km, (d) 192x12.5km, and (e) 384x6.25km.

In the 24x100km system [Fig. 2(a)], we can see that the performance of EDC system (No-OPC) is dominated by the linear ASE noise when the signal power is below -1dBm and increments in the signal power translate into an increment in the Q^2 factor at a rate of $+1\text{dB/dB}$ as expected. The maximum performance ($Q^2 = 14.4\text{dB}$) is reached at 0dBm after which the system enters the nonlinear regime, where the deterministic signal-signal nonlinear noise starts to grow cubically as a function of signal power resulting a degradation of the Q^2 factor with a rate of -2dB/dB . Introducing OPCs into the system results in only partial compensation of the signal-signal nonlinear interactions and enhances the maximum achieved performance Q^2 by 2.5dB, 1.9dB, and 0.6dB for systems with 1-OPC, 2-OPCs, and 3-OPCs, respectively. Figure 2(a) confirms that introducing more OPCs into discretely amplified system with long span length results in a reduction of the performance enhancement compared to that achieved by a single OPC. As the span length is reduced, the performance improves in the linear regime [as ASE noise accumulation is reduced, see Eq. (2)] and degrades in the nonlinear regime which results the system to reach its maximum performance ($Q^2 = 19\text{dB}$) when the span length is shorter than 12.5km. The nonlinear compensation

afforded by OPC increases significantly as the span length reduces, although since the compensation is far from perfect, increasing the number of OPCs continues to degrade the compensated performance. For a 12.5km span length [Fig. 2(d)], the nonlinearity compensation efficiency is sufficiently strong for the competition between signal-noise interaction and imperfect signal-signal compensation to become apparent, with the 2-OPCs and 3-OPC both slightly outperforming the single OPC system by around 1.5dB. For shorter span lengths [e.g. 6.25km, Fig. 2(e)] the nonlinear signal-noise interaction dominates the compensated performance and increasing the number of OPCs enhances of the maximum performance of the system. The theoretical calculations show a good agreement with simulation results, within a margin of error of 0.4dB, at the optimum. However, in the nonlinear regime of Fig. 2(c) and 2(d) an excessive Q^2 degradation slope of -5dB/dB is observed suggesting that a higher order nonlinear interaction has been neglected. We believe that the most likely interaction is the parametric amplification of the uncompensated signal-signal nonlinearities, which could be calculated using a similar approach to the signal-noise interaction. Note that this deviation does not impact theoretical predictions of the simulated system performance at the Q^2 factor at the optimum launch power.

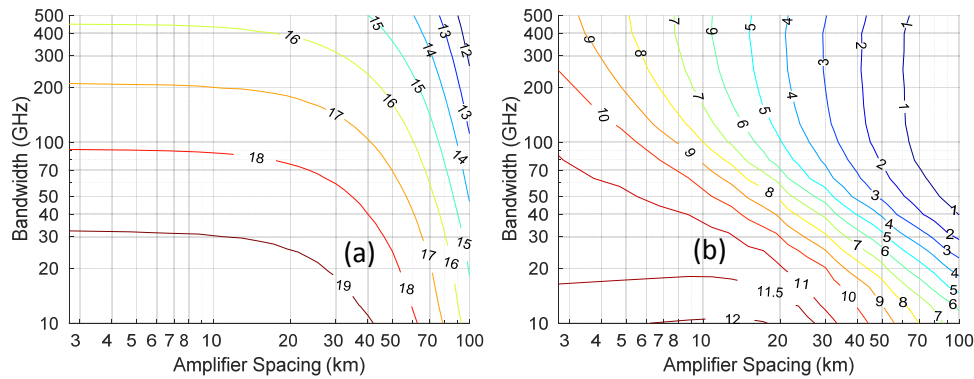


Fig. 3. (a) Maximum Q^2 factor, as a function of span length and bandwidth without OPC compensation. (b) Improvement in the maximum Q^2 factor can be achieved by 1-OPC.

Figure 3 shows the theoretically predicted maximum of Q^2 factor achieved by EDC system (a) and the performance improvement (ΔQ^2) for a single OPC (b) at a total system length of 2400km as a function of amplifier spacing (span length) and signal bandwidth (assuming arbitrary channel baud rate and highly spectrally efficient Nyquist-WDM, baud rate \approx channel spacing). Figure 3 is a result of the numerical calculations of SNR based on Eq. (1)-(4), from which Q^2 ($= \text{SNR}$) is calculated assuming PM-QPSK as a modulation format. Figure 3(a) shows the shorter amplifier spacing (in EDC system) enhances the performance of an optical system at any given optical signal bandwidth; due to the reduction in the accumulated ASE noise along the system which can be concluded from Eq. (2). This performance enhancement due to shortening the amplifier spacing saturates when the amplifier spacing is less than 10km and can reach up to 4.5dB when compared to a system deploying 100km amplifier spacing [18,19]. Figure 3(b) shows that the performance enhancement achieved by mid-link OPC assisted system with long amplifier spacing ($>30\text{km}$) is limited by the partial nonlinear noise compensation efficiency of the OPC, whilst for shorter amplifier spacing ($<30\text{km}$), the improvements tend to saturate, reflecting the nonlinear signal-noise interactions limit. A system that deploys span length longer than 70km barely achieves any more substantial improvement in Q^2 factor than possible using digital nonlinearity compensation ($\sim 1.5\text{dB}$ [8]) for systems with bandwidth above 100GHz.

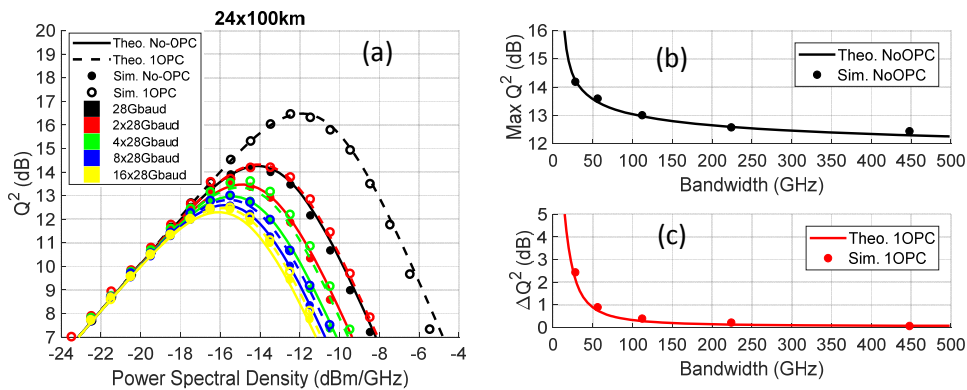


Fig. 4. (a) Q^2 as a function of signal power in 24x100km discretely amplified system. (b) maximum Q^2 achieved by EDC system as a function of the signal bandwidth, (c) Q^2 improvement with mid-link OPC as a function of signal bandwidth.

To visualize the effect of increasing signal bandwidth on the nonlinearity compensation efficiency achieved by the OPC, Fig. 4 which shows the simulated and analytical performance as a function of the number of 28Gbaud channels (28.1GHz WDM channel spacing) for a system with a long amplifier spacing (100km). The simulation results in Fig. 4 shows a good agreement, within 0.3dB margin of error, validating the theoretical predictions made by the closed form approximations presented in Eq. (5) and Eq. (6). As predicted, the maximum Q^2 achieved by EDC system is degraded as a function of signal bandwidth. With an OPC, whilst the performance is always improved the bandwidth dependence is even stronger due to the combined effects of increased nonlinear noise [Eq. (5)] and reduced compensation efficiency [Eq. (6)] as can be clearly seen from Fig. 4(c).

4. Experimental setup and results

To verify the above theory, we implemented a recirculating loop to emulate a discretely amplified transmission system with a span length of 100km, shown in Fig. 5. Eight lasers with linewidths <100 kHz on a 50GHz grid were divided into two bands: Band 1 (Ch1-4), and Band 2 (Ch5-8). The center of the two bands were spectrally separated by 600GHz around a band splitting frequency of 192.72THz. The even and odd indexed channels were separately modulated using dual-polarization optical modulators. Each modulator was fed by a 28Gbaud PM-QPSK (Nyquist roll off = 0.2) electrical signal generated from an arbitrary waveform generator operating at 56GSa/s and a $2^{15}-1$ PRBS bit sequence. The AWG decorrelates the modulating data of X and Y polarizations by 4096 symbols. The two sets of modulated channels (even indexed and odd indexed) were optically decorrelated (4m of optical fiber) and combined by a 3dB coupler. The modulated signals (two WDM bands, each contains 4x28Gbaud PM-QPSK with 50GHz spacing) then were passed to a 2x1 optical switch which was used to fill the recirculating loop. A 3dB coupler was used to split the signal into two copies, one bypassing the OPC and one passing through the OPC to generate the conjugates of the two bands simultaneously. The OPC path contains two extra EDFAs that boost the signal power and balance the conjugated signal powers to the powers at the bypass switch port of the second 2x1 switch. The total gain of the EDFAs matched the total insertion loss of the OPC (16dB in this experiment), including fibre and coupler loss and losses associated with wavelength routing. The second 2x1 optical switch was used to switch between the signals bypassing the OPC and the conjugated signals, to emulate the deployment of mid-link OPC. At the output of the second switch, an EDFA (NF = 6dB) was used to boost the signal power to 20dBm after which the signal's power was controlled by a digitally controlled variable optical attenuator (VOA). After the VOA, signals were passed through 100km standard single mode fiber (Sterlite G.652.D), then an EDFA with 14dBm output power was

used to pre-compensate the insertion loss of the optical switches and the 3dB coupler. At the mid-stage of the booster EDFA, we have used 3-dB splitter to pass the signal both to the loop and to coherent receiver path. A tunable band pass filter (BPF) was used to filter the targeted channels to be detected by the dual polarization coherent receiver (100Gsamples/s). High precision digital delay generators were used to synchronize the optical switches. The captured received signals were then processed using commercial digital signal processing software (Tektronix OM4245) implementing an FIR digital filter, dispersion compensation, 7 tap constant modulus algorithm (CMA), polarization demultiplexing, and decoding. The number of CMA taps were chosen to achieve the highest performance of the detected signals where higher number of taps does not introduce any further performance improvement. In the OPC-assisted system, the dispersion compensation accounted for the residual dispersion resulting from the combination of dispersion slope and wavelength shift from the OPC. The receiver then calculated the BER from the decoded bit sequence, and the EVM from the constellation of the received QPSK symbols.

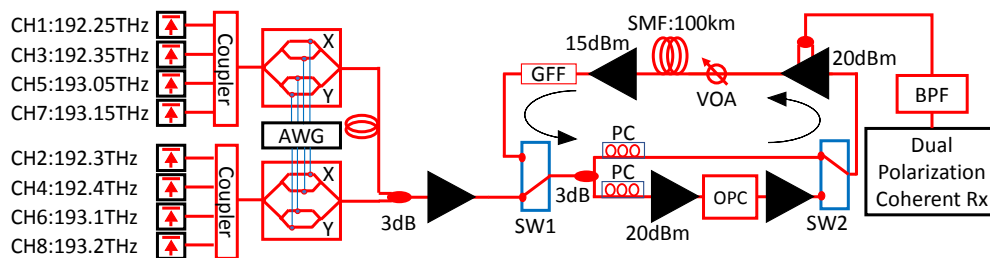


Fig. 5. Experimental setup of OPC-assisted discretely amplified transmission system.

Figure 6(a) shows the dual pump polarization insensitive dual-band OPC, with orthogonally polarized pumps at 1540.4nm and 1570.1nm. The pumps were counter dithered by two tones (60MHz and 600MHz) to combat the Brillouin effect in the highly nonlinear fibre (HNLF) allowing an extra margin of 8dB in launched pump power. The two pump lasers were amplified, filtered using fiber Bragg gratings (FBG), and combined using a polarization beam combiner. A 3-dB splitter was used to generate two copies of the pumps (the power of each copy was 32dBm), and each copy was then combined with one OPC band (split by the input wavelength selective switch into bands located around 1552 and 1559nm). The combinations of pumps and signal bands were counter propagated in a single HNLF ($L = 100\text{m}$, $\lambda_0 = 1557$, $\gamma = 28/\text{W}/\text{km}$, dispersion slope = $0.024\text{ps}/\text{nm}^2/\text{km}$) in order to generate conjugate copies. Finally, the pumps were dumped using bandpass filters, and then the idlers from each path were filtered and combined using a second wavelength selective switch. Figure 6(b) and 6(c) shows the input and output spectrum of the conjugation of the 8 available channels (measured at 1% monitor before and after HNLF for each path). From the figure, we can see that the two signal bands were split (around 1555.7nm) and input ASE noise falls in the idler (conjugate) bands suppressed. We found that the total OPC insertion loss was 16dB including the gain flattening spectral profile. The total signal power injected to the OPC was optimized (20dBm) to achieve minimum penalty on the performance of the conjugated signals. We have seen that the performance of the conjugated signals has a performance penalty of 0.7dB when compared with the back-to-back performance of the modulated signals which was 21.2dB. This implies that the impact of added ASE noise and nonlinearities from the OPC were negligible, especially when compared to the amount of ASE noise and nonlinearities generated within the transmission loop (loop EDFAs and transmission span).

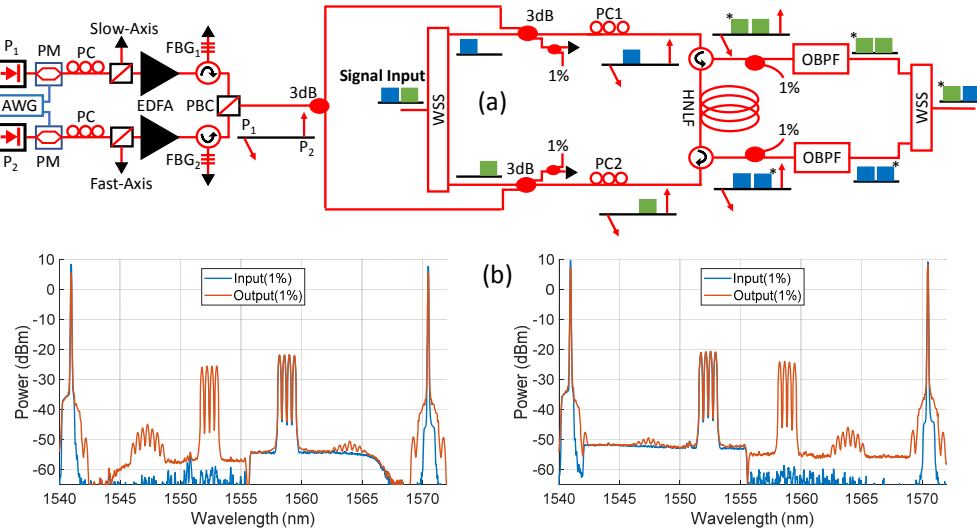


Fig. 6. (a) Experimental setup of dual band, polarization insensitive, dual pump OPC, (b) the optical spectrum measured at the input and output 1% on each signal path.

Figure 7 shows the Q^2 factor, for various number of channels per band measured at a distance of 3000km (with and without OPC), as a function of signal power launched into the fiber (top); the (bottom) of the figure also displays the constellation of the demodulated signals at their maximum performance (optimum signal power). The performance of a channel from each signal band is shown to verify that the performance improvement is balanced across both two bands. The figure compares the experimental Q^2 ($= 1/EVM^2$) with the theoretical SNR Eq. (1) prediction calculated using nonlinear noise from Eq. (5) and Eq. (6). In the theoretical evaluation we have used the following parameters to predict the system performance: $L = 100\text{km}$, $\gamma = 1.3/\text{W/km}$, $\alpha = 0.2\text{dB/km}$, $CD = 16.4\text{ps/nm/km}$, EDFA 1 Gain = 20dB, EDFA 2 Gain = 20dB + attenuation from VOA, amplifier's noise figure = 6dB. The number of spans (N), bandwidth (B_w), and signal launched power (I_s) were changing as will be shown in the following figure. To represent the experimental WDM bandwidth, we have substituted in B_w in the theoretical equations as follows [20]:

$$B_w = B_{ch} M^{2B_{ch}/\Delta f}. \quad (9)$$

where B_{ch} is the bandwidth of the individual channel (which equals the baud-rate 28GHz), Δf is the spectral separation between the adjacent channels, and M is the number of channels *per band*. In the theoretical evaluation, we have ignored the contribution of the nonlinearities from one band to the other as the high phase mismatching (due to the 600GHz separation between the two bands) would degrade the nonlinear interaction efficiency. When two signal channels (single channel per band: CH3 & CH6, $M = 1$) are propagating through the 3000km system, shown in Fig. 7(a) an EDC system (without OPC) reaches its maximum performance (11.4dB) when the signal power is 0.5dBm per channel, on the other hand, the system that deploys mid-link OPC reaches its maximum performance (13.2dB) at 3.5dBm/channel. The 1.8dB improvement (on both channels) in optimum Q^2 achieved by the mid-link OPC is a result of partial nonlinearity compensation of the intra-channel nonlinear interactions; this improvement can be seen from the constellation displayed in the bottom of Fig. 7(a). When increasing the total number of channels to four channels (two channels per band: CH3, CH4, CH5, and CH6, $M = 2$), the improvement in Q^2 achieved by the mid-link OPC is degraded from 1.8dB to 1dB, as shown in Fig. 7(b) both in the curve and the constellation. Finally, an eight-channel system (four channels per band: CH1-8, $M = 4$) further degrades the nonlinearity compensation efficiency leading the improvement in optimum Q^2 achieved by

mid-link OPC system of only 0.7dB, as seen from Fig. 7(c) both in the curve and the constellation. Figure 7 shows that increasing the number of channels propagating through the system not only degrades the optimum Q^2 achieved by EDC system (11.4dB, 11.2dB, and 11dB for 1, 2, and 4 channels per band), but also degrades the nonlinearity compensation efficiency achieved by the OPC causing a degradation in the maximum Q^2 improvement (1.8dB, 1dB, and 0.7dB for 1, 2, and 4 channels per band). The performance of both measured channels (measured in each band) propagating in both systems were close to each other and follow the theoretical predictions within a 0.3dB margin of error. Other experimental results reported in literature (of OPC assisted discretely amplified systems) [21–25] have shown the same trends of the degradation in performance enhancement achieved by OPC when increasing system’s bandwidth.

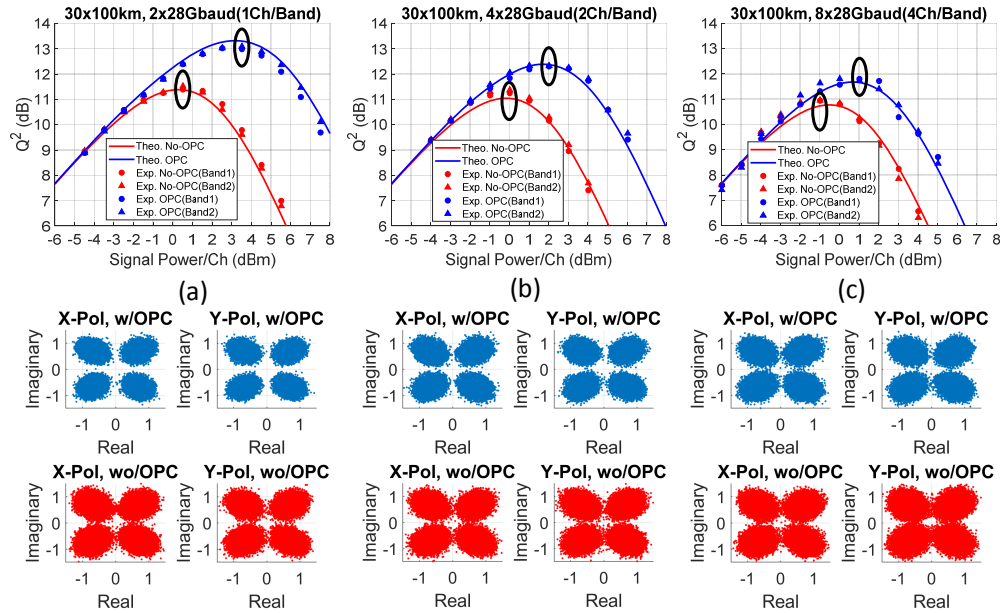


Fig. 7. Q^2 as a function of signal power (top), constellation of received signal at the optimum launch power (bottom); measured at 3000km with and without OPC. The figure contains the results for 2 channels (a), 4 channels (b), and 8 channels (c).

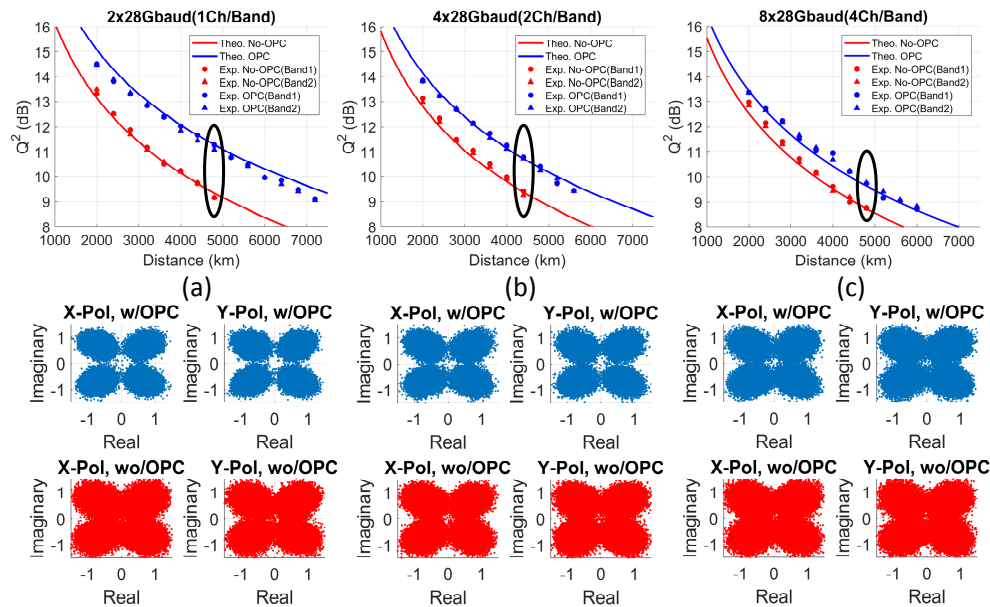


Fig. 8. Q^2 as a function of distance (top), constellation of received signal at the distance marked by the black circle (bottom). The figure contains the results for 2 channels (a), 4 channels (b), and 8 channels (c).

Figure 8 shows Q^2 , for various number of channels per band and measured at the optimum launched signal power for any given distance (with and without OPC) as a function of distance. The bottom of each part of Fig. 8 displays the constellation of the received signals at the distance marked by the black circle in the curve. The figure shows that the performance of mid-link OPC assisted systems are always superior to EDC system. The dual channel system (single channel per band), shown in Fig. 8(a), achieves a reach enhancement of around 45%. As expected, the reach enhancement achieved by OPC assisted system degrades as the bandwidth of the modulated signals increases. The OPC assisted system that delivers 4 channels (2/band) and 8 channels (4/band) achieve reach enhancement ranging around 30% and 20%, respectively; see the curves and constellations in Fig. 8(b) and 8(c). The experimental results show a good agreement with the theoretical predictions, within a margin of error of 0.4dB. The performance uniformity is verified in Fig. 9 which shows the optical spectrum and the BER per channel measured at various distances (shown in the legends, with and without OPC) for the three channel number configurations. Transmission distances were chosen as the last recirculation where the received BER was lower than 2×10^{-3} .

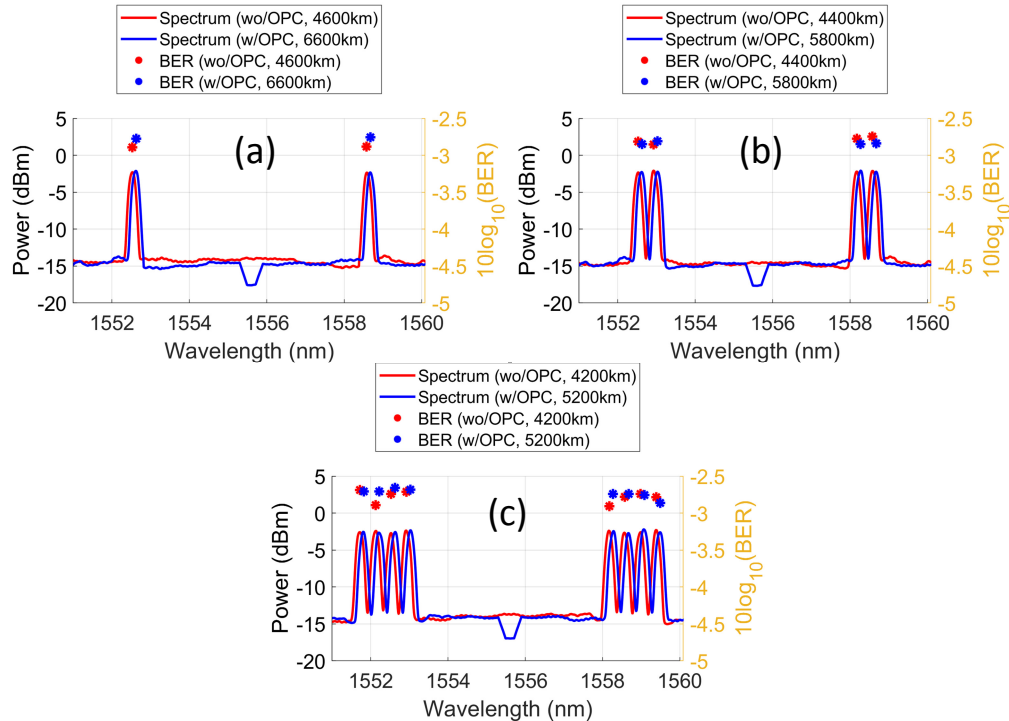


Fig. 9. Optical spectrum and BER per channel at the maximum distance (at which $\text{BER} > 2 \times 10^{-3}$), for 2-channel system (a), 4-channel system (b), and 8-channel system (c); with and without OPC.

Conclusions

We have introduced a closed expression for the residual nonlinear noise compensation efficiency of OPC in discretely amplified systems, validated by simulation and experimental results. Our model shows that the nonlinearity compensation efficiency achieved by mid-link OPC can be degraded significantly as the bandwidth of the modulated signals increases, as observed in other experimental results reported in literature have shown the same trend [21–25]. The bandwidth of the modulated signals identifies the level of dominance of the uncompensated nonlinearities among weakly phase matched signals over the compensated nonlinearities among strongly phase matched signals. The theoretical model, supported by numerical results show that the introduction of multiple OPCs may diminish the nonlinearity compensation efficiency achieved by a single OPC, especially when using large bandwidth optical signals propagating and the large amplifier spacing ($>30\text{km}$). On the other hand, deploying short span lengths can achieve significant compensation signal-signal nonlinear interactions to unveil the signal-noise interaction nonlinear limit. The experimental results, in accordance with the values predicted by the theoretical model, show that OPC enhances the distance reach of discretely amplified transmission system by 43%, 32%, and 24% for $2 \times 112\text{Gbps}$, $4 \times 112\text{Gbps}$, and $8 \times 112\text{Gbps}$ signals.

Original data for this work is available through Aston Research Explorer (<https://doi.org/10.17036/researchdata.aston.ac.uk.00000350>).

Funding

Engineering and Physical Sciences Research Council (EPSRC) (EP/J017582/1 [UNLOC]; EP/L000091/1 [PEACE]); and H2020 Marie Skłodowska-Curie Actions, Marie Curie Fellowship (659950 [INVENTION]).

Acknowledgments

We thank Dr. Marc Stephens (Aston university) for the useful conversations, Sterlite Technologies for providing the transmission fiber, and Finisar for providing a WSS.